

RSC Advances



This is an *Accepted Manuscript*, which has been through the Royal Society of Chemistry peer review process and has been accepted for publication.

Accepted Manuscripts are published online shortly after acceptance, before technical editing, formatting and proof reading. Using this free service, authors can make their results available to the community, in citable form, before we publish the edited article. This *Accepted Manuscript* will be replaced by the edited, formatted and paginated article as soon as this is available.

You can find more information about *Accepted Manuscripts* in the [Information for Authors](#).

Please note that technical editing may introduce minor changes to the text and/or graphics, which may alter content. The journal's standard [Terms & Conditions](#) and the [Ethical guidelines](#) still apply. In no event shall the Royal Society of Chemistry be held responsible for any errors or omissions in this *Accepted Manuscript* or any consequences arising from the use of any information it contains.

1 **Abstract** A novel human immunoglobulin G (HIgG) electrochemical immunosensor
2 was developed based on nanosilver-doped bovine serum albumin microspheres
3 (Ag@BSA). The immunosensor was prepared step-wisely by first modifying the
4 electrode with β -cyclodextrin functionalized gold nanoparticles followed by the
5 immobilization of capture antibodies and then the formation of sandwich-type
6 immunocomplex to introduce Ag@BSA bionanoprobes on the sensor surface. The
7 amplification pathway using the stripping voltammetric measurement of silver ions
8 released from Ag@BSA to monitor the immunoreaction was firstly adopted. The
9 immunosensor exhibited a large dynamic range of 1 fg mL^{-1} to 10 pg mL^{-1} and an
10 ultralow detection limit of 0.5 fg mL^{-1} to HIgG. Moreover, the immunosensor also
11 showed acceptable stability and reproducibility. This biosensor was applied to the
12 detection of the HIgG level in real serum samples.

13 **Keywords:** Electrochemical immunosensor; Bioinspired nanomaterial;
14 β -Cyclodextrin; Immunoglobulin G

15

16 **Introduction**

17 The level of certain biomarkers, such as human immunoglobulin G (HIgG) in
18 serum, can indicate a variety of disease characteristics and provide key information on
19 the humoral immune status^[1,2]. The sensitive determination of important biomarkers
20 is therefore of great significance in clinical research and disease diagnosis.
21 Immunoassay based on the antigen-antibody specific recognition is one of the major
22 analytical techniques in clinical diagnoses^[3]. Among various analytical tools,

1 electrochemical immunosensor has drawn considerable interest not only due to its
2 intrinsic advantages of low cost and simple instruments, but also because of its
3 relatively low detection limit and formidably high sensitivity^[4,5]. The performance of
4 the electrochemical immunosensor was greatly influenced by the electron transfer
5 efficiency and biocompatibility of materials modified on the electrode surface^[6,7].
6 From this point of view, noble metal nanoparticles were frequently chosen for the
7 sensing interface and tracing tags^[3-6]. However, it was a challenge to decrease the
8 background signal produced in the absence of antigens which often restricted the
9 detection limit of the immunosensor^[8-10]. The high background signal, in the vast
10 majority of cases, was caused by the nonspecific adsorption of electroactive labels on
11 the sensing interface^[7,10,11].

12 Bioinspired nanomaterial such as the protein-directed inorganic nanoparticles is a
13 rising-star of nanomaterial. The protein can help to prevent aggregation of
14 nanoparticles and allow the materials to be chemically modified for targeting. The
15 inorganic nanoparticles can exhibit dramatically different structural and electronic
16 properties with the materials synthesized without protein templating. Among them,
17 bovine serum albumin (BSA)-mediated nanomaterial has attracted increasing
18 attention due to green reaction process and multi-functionality of the products^[12-19].
19 BSA-stabilized Pt, Au and Ag nanoclusters have been successfully explored to
20 fabricate sensing interfaces^[14-18]. These nanoclusters provided with some
21 advantageous properties, but not limited to, favorable biocompatibility, excellent
22 conductivity, and enhanced electrocatalytic activity toward oxygen or H₂O₂ reduction

1 [15]. Using Au@BSA or Ag@BSA microspheres as the biomimetic sensing layer, Jia's
2 distinguished group [13,16,17] developed electrochemical biosensor for urinary
3 retinal-binding protein, carcinoembryonic antigen-positive cells and KB cells,
4 respectively. Zhou et al. [12] devised a new sandwich-type electrochemical
5 immunoassay for the detection of carcinoembryonic antigen. The results indicated
6 that the labeled antibody on the Ag@BSA could maintain the native bioactivity for the
7 antigen-antibody reaction. Ma et al [19] expanded the application scope of
8 BSA-stabilized nanomaterials by a 3D origami electrochemical immunodevice. They
9 select Au@BSA nanospheres as nanocarriers for loading numerous metal ions such as
10 Pb^{2+} and Cd^{2+} to form Au@BSA-metal ion tracers. Since nanosilver itself can be
11 electrochemically oxidized at low potential and yield a well-shaped stripping peak [5,8],
12 Ag@BSA can be adopted as desirable labels for electrochemical immunoassay.

13 In this work, Ag@BSA microspheres were applied as the nanocarriers for
14 antibodies, electroactive labels for detection and nanoprobe for signal amplification.
15 As illustrated in Scheme 1, the primary antibodies were immobilized onto the
16 electrode surface via the adsorption and special inclusion ability of β -cyclodextrin
17 functionalized gold nanocomposite (β -CD/Au) [20-24]. Then, Ag@BSA
18 nanocomposites were introduced on the immunosensor surface by the formation of
19 sandwich-type immunocomplex. Dissolution of the silver on the sensor surface gave
20 rise to a "burst" of Ag^+ ions which could produce sensitive peak on the anodic
21 stripping voltammogram. To the best of our knowledge, this is the initial attempt to
22 monitor immunoreaction by anodic stripping voltammetric (ASV) determination of

1 silver ions released from Ag@BSA. With HIgG as a model analyte, the fabricated
2 immunosensor exhibited a low detection limit of 0.5 fg mL⁻¹.

3

4

Scheme 1

5

6 **Experimental**

7 **Materials and reagents**

8 HIgG, mouse anti-HIgG antibody (Ab) and BSA were obtained from Beijing
9 Boisyntesis Biotechnology Co. Ltd. (Beijing, China). Glutaraldehyde (GA) was
10 purchased from Kemiou Chemical Reagent Co. Ltd. (Tianjin, China). β -CD, trisodium
11 citrate and silver nitrate (AgNO₃) were obtained from Shanghai Reagent Company
12 (Shanghai, China). Sodium borohydride (NaBH₄) and Nitric acid (HNO₃) were
13 obtained from Sinopharm Chemical Reagent Co. Ltd. (China). Tween-20 was
14 obtained from MP Biomedicals. All other reagents were of analytical grade and used
15 as received.

16 Phosphate buffered saline (PBS) was prepared with Na₂HPO₄·12H₂O and
17 KH₂PO₄. PBS (0.01M, pH 7.4) containing 1.0% (w/v) BSA and PBS containing
18 0.05% (V/V) Tween-20 (PBST) was used as blocking and washing solution,
19 respectively. Deionized and distilled water was used throughout the study.

20 **Apparatus**

21 All electrochemical experiments were achieved on a CHI660A electrochemical
22 workstation (Shanghai CH Instrument Co. Ltd., China) using a three-electrode system.
23 The working electrode was glassy carbon electrode (GCE) or modified GCE. A

1 saturated calomel electrode (SCE) and a platinum wire served as reference and
2 counter electrode, respectively. UV-vis analysis was performed on UV-2550
3 spectrophotometer (Shimadzu, Japan). Scanning electron microscopy (SEM) images
4 were obtained using a JSM-6390A (JEOL, Japan). FTIR spectrum was conducted on
5 TENSOR-27 FTIR spectrometer (Bruker, GER). The transmission electron
6 microscopy (TEM) images were obtained from Tecnai G² F20 S-TWIN (FEI, USA).

7 **Synthesis of β -CD functionalized Au Nanoparticles**

8 In a typical procedure, 1.0 mL of 0.01M β -CD was mixed with 0.1 mL of 0.01M
9 HAuCl₄ in 3.9 mL of deionized water at room temperature. 0.01 mL of 1.0 M NaOH
10 was injected into the mixture with stirring to adjust to the pH 10.5 of a solution. After
11 being vigorously stirred, the mixture was continuously heated at 60°C for 3 hours in a
12 water bath. The color of the solution was transferred from pink to wine red, indicating
13 to the formation of AuNPs. UV-vis spectrum of β -CD/Au (Figure S1) was in
14 accordance with a previous report^[24].

15 **Synthesis of Ag@BSA microspheres**

16 Ag@BSA microspheres were synthesized using a slightly modified recipe by
17 Jia's group^[13]. Initially, at room temperature, 5mL of 0.05 M AgNO₃ solution was
18 added to 10 mL of 3.0 mg mL⁻¹ BSA solution under stirring, and then the mixture kept
19 static under N₂ for 5 hours. Afterward, 0.2 mL of hydrazine monohydrate solution was
20 rapidly injected into the mixture and continuously stirred. After being stirred for 30
21 min, the mixture was aged at room temperature for 48 h. Then, the resulting solution
22 was centrifuged at 5000 rpm for 10 min. Finally, the obtained product was

1 re-dispersed in deionized water and stored at 4 °C before use.

2 **Conjugation of Ag@BSA microspheres with detection antibody**

3 The conjugation of detection antibody (Ab₂) on Ag@BSA microspheres were
4 prepared by this protocol. 600 μL of GA solution (excess) was dispersed into 4.0 mL
5 of Ag@BSA suspension (1.0 mg mL⁻¹) under vigorous stirring, following by
6 incubation at room temperature overnight. The excess GA was removed by
7 centrifugation and the obtained sample was redispersed in 2.0 mL of 0.5 M Na₂CO₃.
8 Afterwards, 100 μL of Ab₂ (100 μg mL⁻¹) were injected into the mixture and stirred
9 for 10 min, the mixture was transferred to the refrigerator at 4 °C for further reaction
10 (overnight). During this process, antibodies were covalently conjugated onto the
11 surface of Ag@BSA microspheres. Finally, the suspension was separated by
12 centrifugation (8000 rpm, 10 min) and redispersed in 4.0 mL of 0.01M PBS (pH7.4).

13 **Preparation of the electrochemical immunosensor**

14 In order to prepare the modified electrode, 5 μL of β-CD/Au dispersion was
15 coated on the GCE. After dried, 5 μL of 0.2 mg mL⁻¹ anti-Human IgG (Ab₁) was
16 dropped on the surface of β-CD/Au/GCE, which was incubated at 4 °C overnight. The
17 excess antibodies were removed with PBST and PBS. Finally, a drop of 5 μL blocking
18 solution was covered on the electrode surface and incubated for 30 min at 37 °C to
19 block possible remaining active sites against nonspecific adsorption. After another
20 washing with PBST and PBS, the immunosensor was obtained and stored at 4 °C
21 prior to use.

22 **Measurement procedure**

1 To carry out the immunoreaction and electrochemical measurement, the
2 immunosensor was incubated at 37 °C for 30 min with different concentration of
3 HIgG. After washing, the immunosensor was further incubated with a certain volume
4 of Ag@BSA-Ab₂ for 40 min at 37 °C. After rinsing, the silver ions were released by
5 adding 200 µL of 1.5M HNO₃ and quantified by ASV at following conditions: 10 min
6 deposition at -0.5 V, and potential scan at the linear sweep voltammetry (LSV) from
7 -0.3 to 0.3 V at 50 mV s⁻¹ was performed in a cell containing 5.0 mL of 0.6 M KNO₃
8 as the electrolyte solution to record the response.

9

10 **Results and discussion**

11 **Characterization of Ag@BSA microspheres**

12

13

Figure 1

14 To study the pictorial presentation of the silver nanoparticles in solution, UV-vis
15 spectrum of Ag@BSA was recorded (Figure 1A). A broad peak at around 440 nm was
16 observed, which is consistent with the previous reporting for the surface plasmon
17 peak of Ag@BSA microspheres [25,26]. The structure of the microspheres was further
18 characterized by the techniques of SEM (Figure 1B, C) and TEM (Figure 1D). The
19 uniform microspheres with a mean size of 500 nm in diameter and rough surface were
20 acquired. The functional groups on the large surface of Ag@BSA make the
21 microspheres appropriate for the covalent attachment of antibodies [16,17].

22 **Characteristics of the immunosensor and signal amplification**

23 The impedance change of the interfacial property of the electrode was

1 characterized using electrochemical impedance spectroscopy (EIS). It is well known
2 that the semicircle portion of Nyquist plot at high frequencies represents electron
3 transfer-limited process, where the diameter equals the electron transfer resistance [4].
4 As shown in Figure 2A, bare GCE displayed an ultra-small semicircle (curve a),
5 suggesting a characteristic of diffusion-limit step of the electrochemical process [27].
6 After β -CD/Au was modified on the surface of the GCE (curve b), the semicircle
7 diameter increased slightly compared with bare GCE, which demonstrated the
8 excellent electronic conductivity of β -CD/Au. EIS of β -CD modified electrode was
9 also recorded. The diameter of the semicircle (shown in curve c) was apparently
10 bigger than that for β -CD/Au/GCE, demonstrating that the nanogold plays an
11 important role in facilitating the electron exchange between the solution and the
12 electrode. The diameter increased consecutively with the immobilization of Ab₁
13 (curve d), the incubation of HIgG (curve e) and then Ab₂-Ag@BSA (curve f),
14 indicating that the immunocomplex had formed on the electrode surface and thus
15 hindered the electron transfer.

17 Figure 2

18
19 The release of Ag⁺ from Ag@BSA microspheres following the immunoassay
20 sandwich formation was firstly adopted to quantitatively monitor the immunoreaction.
21 Figure 2B depicts the anodic stripping voltammetric curves of this immunosensor
22 toward blank buffer and HIgG, respectively. As shown in curve a, the immunosensor
23 incubated with blank buffer gave rise to a small peak which was produced by the

1 nonspecific adsorption of Ag@BSA on the electrode surface. The peak current is only
2 about 4.2 μA , which is negligible compared with the response for 10 pg mL^{-1} HIgG
3 shown in curve b, Figure 2B, where a well-defined stripping peak at 0.18 V,
4 corresponds to the oxidation of Ag^[23, 28], was observed. The peak current increased
5 when the concentration of target protein increased from 10 pg mL^{-1} to 500 pg mL^{-1}
6 (curve c, Figure 2B), indicating that the Ag@BSA microspheres-based strategy is
7 appropriate for the quantitative detection of HIgG.

8 **Optimization of experimental conditions**

9 The preconcentration step is critical in any stripping technique, and thus we
10 investigated the effect of silver accumulation time on immunosensor response. As
11 shown in Figure 3A, the peak current on ASV of enriched silver increased linearly
12 when the silver accumulation time was varied from 1 to 30 min. Considering both
13 sensitivity and analytical time, we chose 10 min for the optimized silver enrichment.

14

15

Figure 3

16

17 The concentration of capture antibody was optimized. As shown in Figure 3B,
18 when the concentration of anti-HIgG changed from 0.05 to 0.5 mg mL^{-1} , the peak
19 current increased till it nearly reached a plateau at 0.2 mg mL^{-1} . The possible reason
20 for the trend was that more antigen-binding sites were accessible when more
21 antibodies were immobilized. Higher concentration than 0.2 mg mL^{-1} of antibodies
22 might increase disorder in alignment of adsorbed antibody and steric hindrance of
23 immunoreaction^[27]. So, 0.2 mg mL^{-1} Ab₁ was selected for the following experiments.

1 The effect of the incubation time for HIgG and Ab₂-Ag@BSA was also investigated.
2 As shown in Figure 3C, the ASV response of the immunosensor increased with an
3 increment of incubation time and tended to level off at 40 min, which showed the
4 saturated state of the sandwich immunoreactions. Therefore, the incubation time of 40
5 min was adopted as the optimal condition in this work.

6 **Analytical performance**

7 Under optimal conditions, ASV was used to investigate the relationship between
8 the peak current values and HIgG concentration. The ASV response of the
9 immunosensor for HIgG measurement increased with increasing the concentration of
10 the analyte (Figure 5). The calibration plot showed two linear segments between the
11 peak currents and the logarithm of analyte concentrations in the range from 1 fg mL⁻¹
12 to 10 pg mL⁻¹ (Figure 5B). And the equations were $I = 56.31 + 14.33 \lg C$ (pg mL⁻¹)
13 with a correlation coefficient of 0.994 and $I = 18.01 + 46.97 \lg C$ (pg mL⁻¹) with a
14 correlation coefficient of 0.997, respectively. Some previous immunosensors [29,30] and
15 voltammetric analysis [31] also exhibited two slopes of calibration curves. For this
16 work, the possible reason for the presence of two linear ranges was that the
17 accumulation of the conductive Ag@BSA microspheres with the high concentration
18 of HIgG enhanced the charge transfer in electrochemical oxidation of nanosilver, and
19 therefore improved the sensitivity of the immunoassay. The detection limit was
20 estimated to be 0.5 fg mL⁻¹ at a signal-to-noise of 3. Based on the comparison listed in
21 Table 1, we can find that this immunosensor exhibited an ultralow detection limit
22 which is one order of magnitude lower than the previous immunosensor using

1 ferrocene tagged peptide nanowire as probes^[9] or thionine doped mesoporous ZnO^[32],
2 and was much lower than that of the immunosensor based on in situ deposited
3 polyaniline^[33] or gold nanoparticles^[34], as well as the newly-reported label-free
4 electrochemical immunosensor^[4, 35].

5 **Figure 4**

6 **Table 1**

7 To evaluate specificity of the developed immunosensor for the detection of HIgG,
8 the immunosensor was incubated with several other low-abundance proteins in serum
9 such as hemoglobin (10 pg mL⁻¹), human serum albumin (10 pg mL⁻¹), BSA (1%). As
10 depicted from Figure 5, the current response for the target analyte was much higher
11 than those of others, indicating that the immunosensor possesses a good selectivity in
12 detecting HIgG.

13

14 **Figure 5**

15

16 The stability of Ag@BSA and Ag@BSA-antibodies are both good. Ag@BSA
17 particles dispersed in aqueous solution remained their initial shape and particles size
18 after twelve months storage in 4°C. Ag@BSA-antibodies can be applied for the
19 immunosensing within three months of storage in 4°C. And the ASV signal of the
20 immunosensor for 0.1 ng mL⁻¹ of HIgG retained 96% of its initial current after the
21 electrode was stored at 4°C for four weeks. The good stability of the immunosensor
22 was contributed to the good biocompatibility and effective antibody immobilization of
23 Ag@BSA.

24

1 **Analysis of real samples**

2 The determination of HIgG in human serum sample was employed by standard
3 addition method to demonstrate the practical application of the proposed
4 immunosensor. The results were summarized in Table 2. It showed that the recovery
5 ranged from 91.3% to 109.0% and the RSD was from 3.3% to 5.9%. These results
6 indicated acceptable reliability of the method for practical applications.

7

8

Table 2

9

10 **Conclusions**

11 In this work, a novel sandwich-type immunosensor for sensitive electrochemical
12 determination of HIgG was constructed. Ag@BSA microspheres worked as the
13 antibody carriers and electroactive probes. The immunosensor exhibited an ultralow
14 detection limit, wide dynamic range and satisfied recovery in human serum. Therefore,
15 this method provides a promising strategy for protein biomarker determination in
16 clinical applications.

17 **Acknowledgement**

18 The authors gratefully acknowledge the financial support of the National Science
19 Foundation of China (No. 21275116).

20

21

22

23 **References**

- 1 [1] M. A. Slatter and A. R. Gennery, *Clin. Exp. Immunol.* 2008, 152, 389–96.
- 2 [2] A. R. Gonzalez-Quintela, A. F. Gude, J. Campos, J. Rey, L. M. Meijide, et al.,
3 *Clin. Exp. Immunol.* 2008, 151, 42–50.
- 4 [3] R. Li, K. B. Wu, C. X. Liu, Y. Huang, Y. Y. Wang, H. G. Fang, et al., *Anal.*
5 *Chem.*, 2014, 86, 5300–5307.
- 6 [4] L Liu, Y Li, L Tian, T Guo, W Cao, Q Wei, *Sens. Actuators B*, 2015, 211,
7 170–176.
- 8 [5] G. S. Lai, L. L. Wang, J. Wu, H. X. Ju, F. Yan, *Anal. Chim. Acta*, 2012, 721, 1–6.
- 9 [6] S Weng, Q Liu, C Zhao, G Hong, Z Jiang, L Lin, *Sens. Actuators B*, 2015, 216,
10 307–315.
- 11 [7] B. V. Chikkaveeraiah, A. A. Bhirde, N. Y. Morgan, H. S. Eden, X. Chen, *ACS*
12 *Nano*, 2012, 6, 6546–6561.
- 13 [8] L. Ma, D. Ning, H. Zhang, J. Zheng, *Biosens. Bioelectron.*, 2015, 68, 175–180.
- 14 [9] Y. Y. Ding, D. Li, B. Li, K. Zhao, W. Du, J. Y. Zheng, et al., *Biosens.*
15 *Bioelectron.* 2013, 48, 281–286.
- 16 [10] S. H. Jenkins, W. R. Heineman, H. B. Halsall, *Anal. Biochem.* 1988, 168,
17 292–299.
- 18 [11] G. Lai, H. Zhang, J. Yong, A. Yu, *Biosens. Bioelectron.* 2013, 478, 178–183.
- 19 [12] J. Zhou, J. Tang, G. N. Chen, D. P. Tang, *Biosens. Bioelectron.*, 2014, 54,
20 323–328.
- 21 [13] C. Y. Hu, D. P. Yang, Z. H. Wang, P. Huang, X. S. Wang, D. Chen, D. X. Cui, M.
22 Yang and N. Q. Jia, *Biosens. Bioelectron.*, 2013, 41, 656–662.

- 1 [14]S. B. He, H. H. Deng, A. L. Liu, G. W. Li, X. H. Lin, W. Chen, X. H. Xia,
2 ChemCatChem, 2014, 6, 1543–1548.
- 3 [15]C. Y. Hu, D. P. Yang, F. J. Zhu, F. J. Jiang, S. Y. Shen, J. L. Zhang, ACS Appl.
4 Mater. Interfaces, 2014, 6, 4170–4178.
- 5 [16]C. Y. Hu, D. P. Yang, Z. Y. Wang, L. L. Yu, J. L. Zhang, N. Q. Jia, Anal. Chem.,
6 2013, 855, 200–5206.
- 7 [17]C. Y. Hu, D. P. Yang, K. Xu, H. M. Cao, B. N. Wu, D. X. Cui, N. Q. Jia, Anal.
8 Chem., 2012, 84, 10324–10331.
- 9 [18]H. M. Cao, D. P. Yang, D. X. Ye, X. X. Zhang, X. E. Fang, S. Zhang, B. H. Liu, J.
10 L. Kong, Biosens. Bioelectron., 2015, 68, 329–335.
- 11 [19]C. Ma, W. P. Li, Q. K. Kong, H. M. Yang, Z. Q. Bian, X. R. Song, J. H. Yu, M.
12 Yan, Biosens. Bioelectron., 2015, 63, 7–13.
- 13 [20]J. Gao, Z. K. Guo, F. J. Su, L. Gao, X. H. Pang, W. Cao, B. Du, Q. Wei, Biosens.
14 Bioelectron. 2015, 63, 465–471.
- 15 [21]Q. F. Li, D. P. Tang, F. M. Lou, X. M. Yang, G. N. Chen, 2014, 1, 441–447.
- 16 [22]X. Wang, X. Li, C. Luo, M. Sun, L. Li, H. Duan, Electrochim. Acta, 2014, 130,
17 519–525.
- 18 [23]J. Wen, S. Zhou, Y. Yuan, Biosens. Bioelectron., 2014, 52, 44–49.
- 19 [24]T. Huang, F. Meng, L. M. Qi, J. Phys. Chem. C, 2009, 113, 13636–13642.
- 20 [25]A. Gebregeorgis, C. Bhan, O. Wilson, D. Raghavan, J. Colloid Interface Sci.,
21 2013, 389, 31–41.
- 22 [26]P. Huang, D. P. Yang, C. Zhang, J. Lin, M. He, L. Bao, D. Cui, Nanoscale, 2011,

- 1 3, 3623–3626.
- 2 [27]G. Wang, X. Gang, X. Zhou, G. Zhang, H. Huang, X. Zhang, L.Wang, *Talanta*,
- 3 2013, 103, 75–80.
- 4 [28]Y. Zhu, P. Chandra, Y. B. Shim, *Anal. Chem.*, 2013, 85, 1058–1064.
- 5 [29]D. Feng, L. Li, X. Fang, X. Han, Y. Zhang, *Electrochim. Acta*, 2014, 127,
- 6 334–341.
- 7 [30]X. Gao, Y. Zhang, Q. Wu, H. Chen, Z. Chen, X. Lin, *Talanta*, 2011, 85,
- 8 1980–1985.
- 9 [31]Y. Fan, J.H. Liu, C.P. Yang, M. Yu, P. Liu, *Sens. Actuators B*, 2011, 157,
- 10 669–674
- 11 [32]X. Cao, S. Liu, Q. Feng, N. Wang, *Biosens. Bioelectron.*, 2013, 49, 256–262.
- 12 [33]G. Lai, H. Zhang, T. Tamanna, A. Yu, *Anal. Chem.*, 2014, 86, 1789–1793.
- 13 [34]G. Lai, H. Zhang, J. Yong, A. Yu, *Biosens. Bioelectron.*, 2013, 47, 178–183.
- 14 [35]N. Wang, C. Gao, Y. Han, X. Huang, Y. Xu, X. Cao, *J. Mater. Chem. B*, 2015, 3,
- 15 3254–3259.
- 16
- 17
- 18
- 19
- 20
- 21
- 22

1

2

Table 1 Comparison of the analytical performance of some immunosensors for

3

detection of HIgG

| Sensing platform* | Linear range (pg mL ⁻¹) | Detection limit (pg mL ⁻¹) | Ref. |
|--|--|---|-----------|
| GCE/AuNPs-GN-Ab ₁ /HIgG/Ab ₂ -PNW-Fc | 0.01–100 | 0.005 | [9] |
| GCE/AgNW-Chit/Ab ₁ /HIgG/HRP-Ab ₂ -ZnO-TH | 10–200000 | 4 | [32] |
| SPCE/GN/AuNPs/Ab ₁ /HIgG/ Au NP-Ab ₂ -HRP | 20–500000 | 9.7 | [33] |
| SPCE/CNT-Ab ₁ /HIgG/Ab ₂ -AuNPs-PDA/silica | 10–10000 | 6.9 | [34] |
| GCE/GN-CNTs-Pd/ Ab ₁ /HIgG | 10–25000 | 3.3 | [4] |
| GCE/CuSNWs-Chit/Ab ₁ /HIgG (AA in solution) | 1-320000 | 0.1 | [35] |
| GCE/ β-CD-AuNPs /Ab ₁ /HIgG/Ab ₂ -BSA@Ag | 0.001–10 | 0.0005 | This work |

4

* SPCE: screen-printed carbon electrode; GN: graphene; PNW-Fc: ferrocene-peptide nanowire; AgNW: silver

5

nanowire; HRP: horseradish peroxidase; TH: thionine; Chit: chitosan; PDA: polydopamine; CNTs: carbon

6

nanotubes; CuSNWs: CuS nanowires; AA: ascorbic acid.

7

8

9

10

11

12

13

14

Table 2 Results of serum sample assay and recoveries (n=3)

| Initial HIgG in sample | | Measured after addition | | | |
|-----------------------------|-----------------|---------------------------------|---------------------------------|-----------------|--------------|
| C (pg mL ⁻¹) | RSD (%, n=5) | Added (pg mL ⁻¹) | Found (pg mL ⁻¹) | Recovery (%) | RSD (n=5) |
| 410.00 | 2.6 | 0.1 | 410.11 | 109.0 | 5.9 |
| | | 10 | 419.13 | 91.3 | 3.3 |
| | | 500 | 892.73 | 96.5 | 4.6 |

15

1

2

3 **Figure captions**

4 **Scheme 1.** Illustration for preparation of β -CD/Au (A), nanolabels (B) and the
5 immunosensor

6 **Figure 1.** UV-vis spectrum (A), SEM (B, C) and TEM (D) images of Ag@BSA.

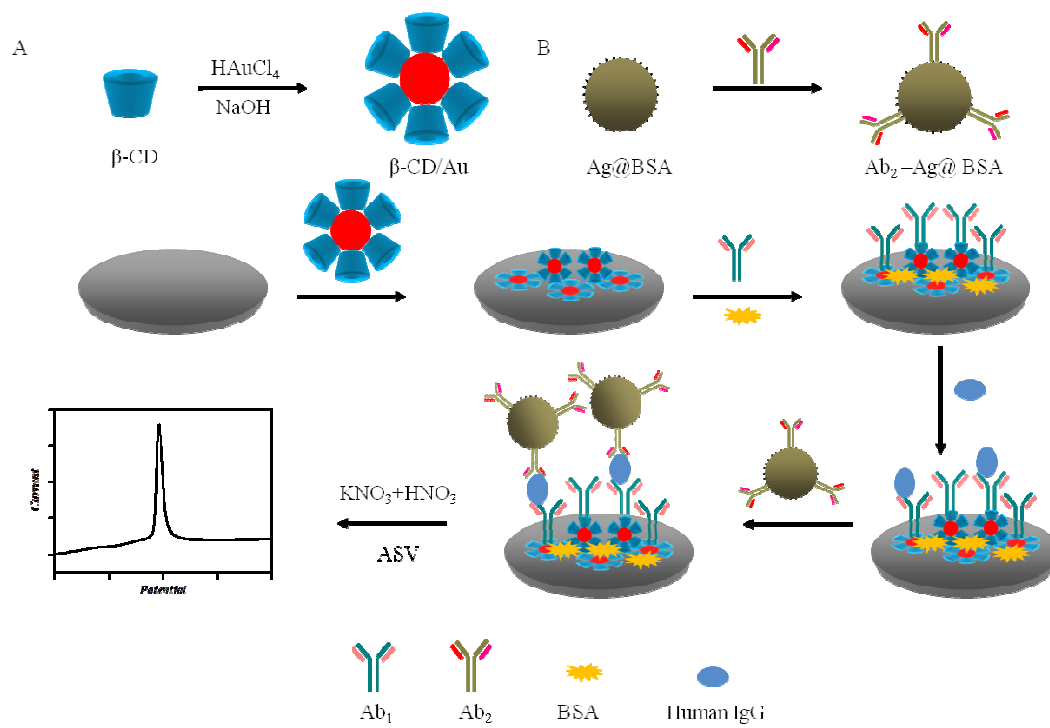
7 **Figure 2.** (A) EIS obtained for different modified electrodes in KCl solution
8 containing 0.5 mM $\text{Fe}(\text{CN})_6^{3-}/\text{Fe}(\text{CN})_6^{4-}$. (a) GCE, (b) β -CD-Au /GCE, (c)
9 β -CD/GCE, (d) Ab_1/β -CD/Au/GCE, (e) HlgG/BSA/ Ab_1/β -CD-Au/GCE, (f)
10 Ab_2 -Ag@BSA/HlgG/BSA/ Ab_1/β -CD/Au/GCE. (B) ASV of the immunosensor after
11 sandwich immunoreactions with blank control (a), 10 pg mL^{-1} (b) and 500 pg
12 mL^{-1} HlgG (c) in 0.6 M $\text{KNO}_3/1$ M HNO_3 solution. Deposition potential: -0.5V;
13 deposition time: 10 min; scan rate: 50 mV s^{-1} .

14 **Figure 3.** Dependence of stripping peak current of the immunosensor on (A)
15 incubation time on the amount of silver enrichment, (B) antibody concentration (C)
16 incubation time for the antigen-antibody.

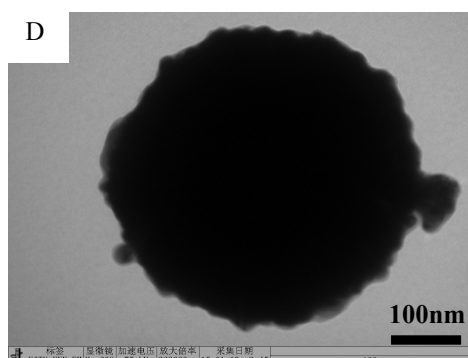
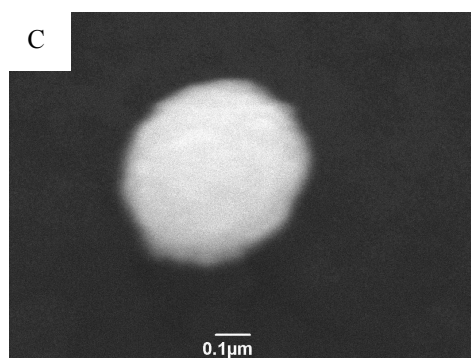
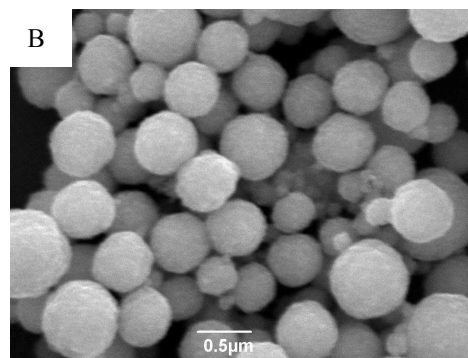
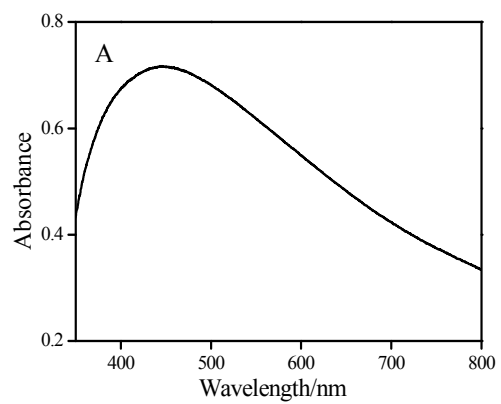
17 **Figure 4.** ASVs of the immunosensing system incubated in HlgG solution with
18 different concentrations (A) and calibration curves for HlgG determination (B) ($n=3$
19 for error bars).

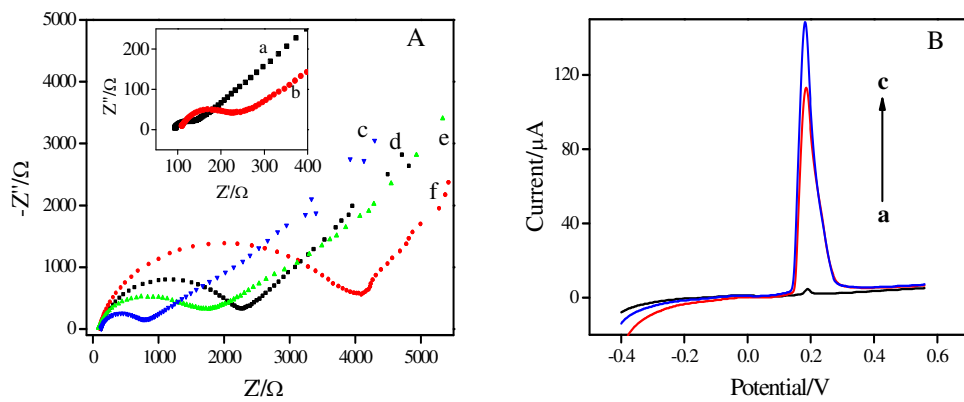
20 **Figure 5.** ASV response of the immunosensor to blank control, 10 pg mL^{-1} Hb, 10 pg
21 mL^{-1} HSA, 1% BSA and 0.1 ng mL^{-1} HlgG.

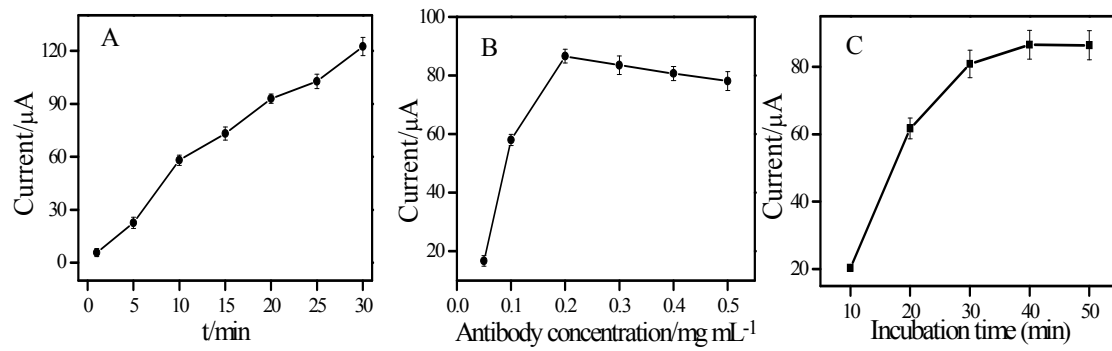
22

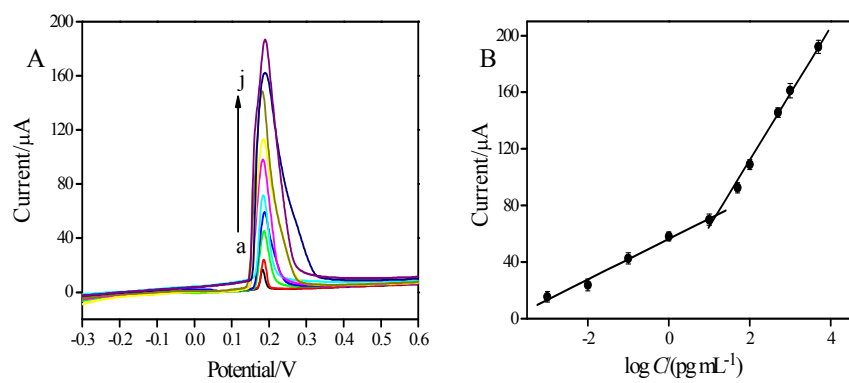


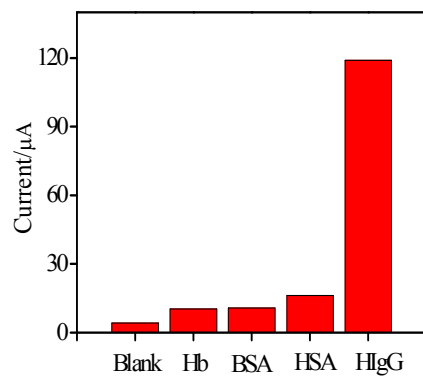
C

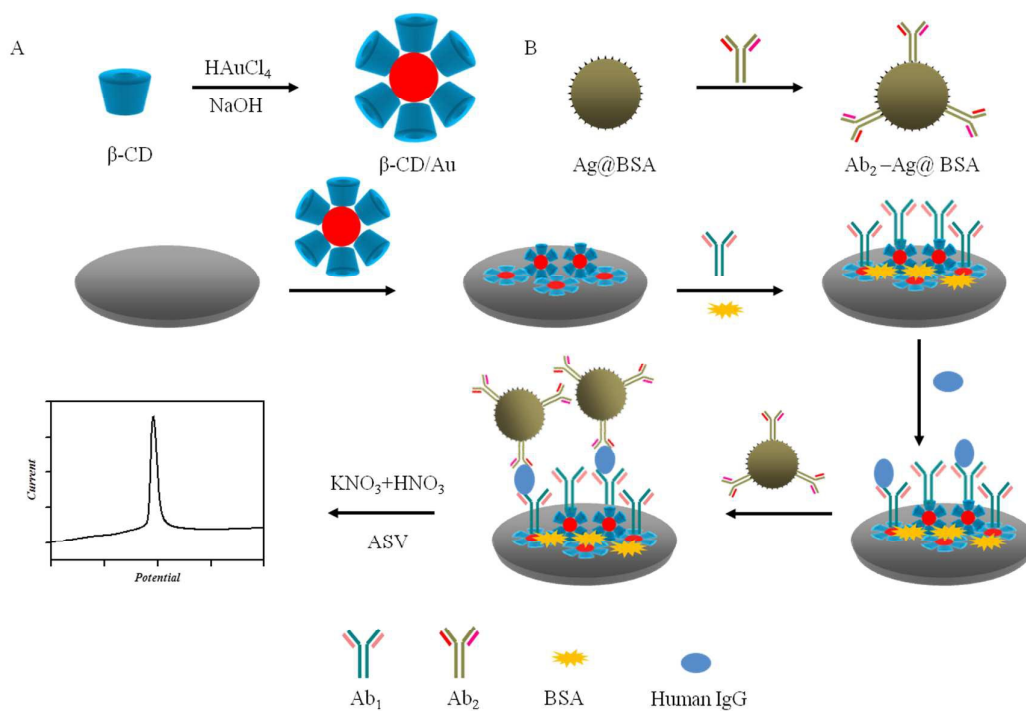












Ag@BSA microspheres were applied as the electroactive labels for signal amplification and the ultimate immunosensor exhibited an ultralow detection limit.